STScI | SPACE TELESCOPE SCIENCE INSTITUTE

JWST TECHNICAL REPORT

Title: NIRISS Commissioning Results: NIS-015 – NIRISS GR150C/R Flux Calibration (NGAS CAR-699, APT 1089)	Doc#: JWST-STScI-008328, SM-12 Date: 7 December 2022 Rev: -
Authors: Swara Ravindranath, Kevin Volk, and the NIRISS team Phone: 410-338-2427	Release Date: 4 January 2023

1 Abstract

This report presents analysis and results of commissioning program NIS-015 (NGAS CAR-699, APT 1089). We describe the observations, data reduction and analysis to determine the flux calibration for the GR150R and GR150C grisms in the NIRISS WFSS mode. The flux measurement was made for each grism crossed with the six blocking filters used for the NIRISS WFSS mode. The observations were taken with two flux standard stars, WD1657+343 located in the center of the detector in the full array, and P330E located in the WFSS64R/C subarrays. The observed count-rates as a function of wavelength were compared with the fluxes in the flux-calibrated standard spectra to determine the sensitivity function. The results from the program were also compared to the pre-flight count-rates from the JWST exposure time calculator to revise the reference files for the ETC. The reference files for NIRISS WFSS flux calibration were created and delivered to CRDS for use in the JWST calibration pipeline.

2 Introduction

The NIRISS Wide-Field Slitless Spectroscopy (WFSS) mode is enabled by two identical (R~150) grisms GR150R and GR150C which are mounted on the Filter Wheel (FW). The grisms are crossed with one of the 6 blocking filters (F090W, F115W, F140M, F150W, F158M, and F200W) in the Pupil Wheel (PW) to obtain the dispersed images of astronomical sources. The WFSS science uses the spectral orders +1 for the six filters which cover the wavelength range from 0.8 – 2.2 microns that need to be wavelength and flux calibrated, along with the +2 spectral order for the F090W filter (Ravindranath 2014a,b). The NIS-015 commissioning program to perform the WFSS flux calibration was done by observing two flux standard stars in 3 visits during May 22-23, 2022 using APT program 1089 (see Table 1 for details). The standard star WD1657+343 (spectral type DA1; K=17.6 Vega magnitude) was observed with the GR150C and R grisms crossed with each of the 6 blocking filters using the FULL array. In the special requirements an offset of (6.3101”, -0.6635”) was applied to match the NIS_WFSS SIAF aperture and ensure that the direct and dispersed images do not fall on the rows separating the detector channels. The 4-point large WFSS dither pattern was chosen to mitigate the effects of persistence. The flux standard

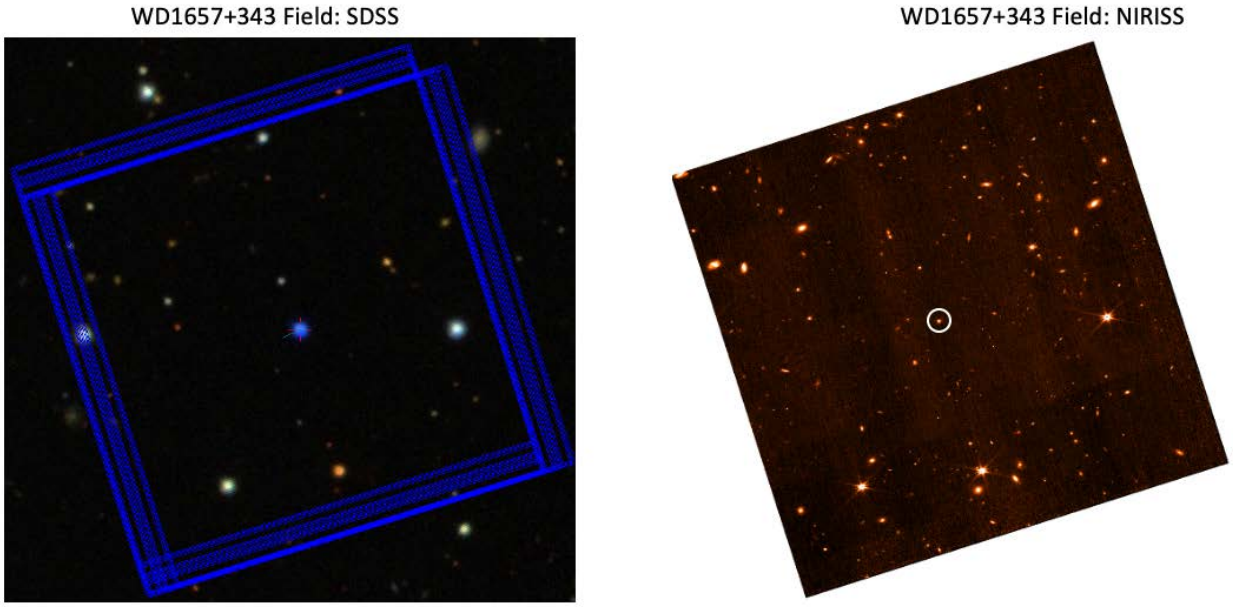

Figure 1: The target field for the flux standard WD1657+343. Left panel shows the Sloan Digital Sky Survey (SDSS) image with the star marked by red cross-wire, while the right panel shows the NIRISS F200W image taken in the FULL array mode with the star marked with a white circle.

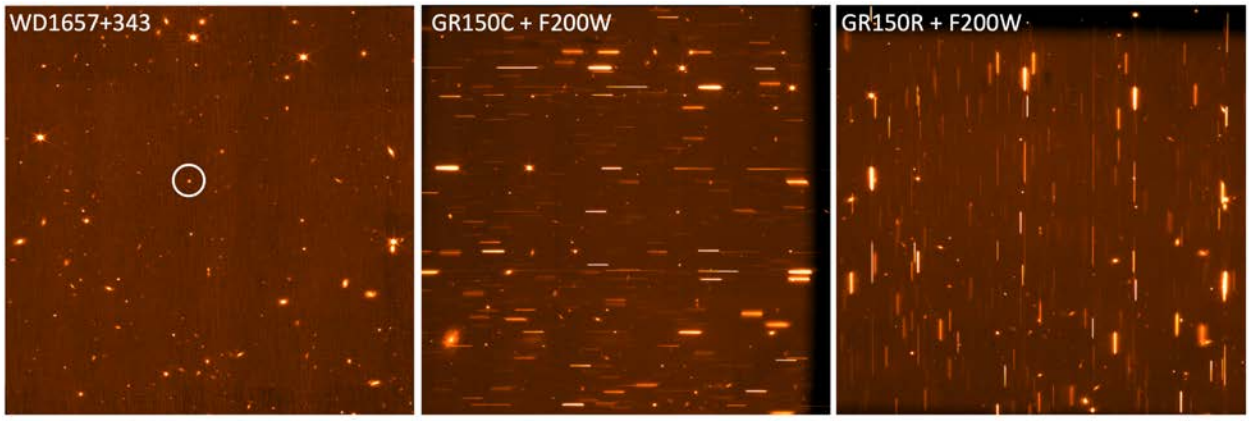

Figure 2: The direct and dispersed images for the WD1657+343 field in full array. The direct image (left) shown here was taken using the F200W filter, and the same filter crossed with GR150C (middle) and GR150R (right) are shown in the other panels. The star WD1657+343 is marked with white circle in the left panel. The field of view shown is 2.2 arcmins x 2.2 arcmins.

star was also intended to be used for the trace measurements because it was isolated in the SDSS images, but the depth of the observed NIRISS images revealed many galaxies (Figure 1). The direct and dispersed images are shown in Figure 2 for GR150R and GR150C crossed with the F200W grism. The standard star P330E (spectral type G0V; K=11.4 Vega magnitude) was observed using the WFSS64R, WFSS64C subarrays with the grisms crossed with the wide bands (F090W, F115W, F150W, and F200W) using 2-point small dithers. The star P330E was selected to tie in the flux calibration for the blue and red wavelength ranges of NIRISS and NIRCam grisms.

Figure 3: The dispersed image for the standard star P330E taken in the subarray WFSS64C using the GR150C grism crossed with the F200W filter. The curvature of the spectral trace becomes noticeable going from the -2 order (right) to the +2 order (left).

Table 1: Details of the observations from program APT 1089

FITS file root ID	Pupil	Filter	Subarray	Dithers	Ngroups	Nints	Duration (seconds)
Target: WD1657+343, Observation / Visit 1							
jw01089001001_32101	F090W	CLEAR	FULL	1	5	1	64.421
jw01089001001_33101	F090W	GR150R	FULL	4	20	1	225.473
jw01089001001_34101	F090W	CLEAR	FULL	2	5	1	128.842
jw01089001001_35101	F090W	GR150C	FULL	4	20	1	225.473
jw01089001001_36101	F090W	CLEAR	FULL	1	5	1	64.421
jw01089001001_26101	F115W	CLEAR	FULL	1	5	1	64.421
jw01089001001_27101	F115W	GR150R	FULL	4	20	1	225.473
jw01089001001_28101	F115W	CLEAR	FULL	2	5	1	128.842
jw01089001001_29101	F115W	GR150C	FULL	4	20	1	225.473
jw01089001001_30101	F115W	CLEAR	FULL	1	5	1	64.421
jw01089001001_08101	F150W	CLEAR	FULL	1	5	1	64.421
jw01089001001_09101	F150W	GR150R	FULL	4	20	1	225.473
jw01089001001_10101	F150W	CLEAR	FULL	2	5	1	128.842
jw01089001001_11101	F150W	GR150C	FULL	4	20	1	225.473
jw01089001001_12101	F150W	CLEAR	FULL	1	5	1	64.421
jw01089001001_02101	F200W	CLEAR	FULL	1	5	1	64.421
jw01089001001_03101	F200W	GR150R	FULL	4	30	1	332.841
jw01089001001_04101	F200W	CLEAR	FULL	2	5	1	128.842
jw01089001001_05101	F200W	GR150C	FULL	4	30	1	332.841
jw01089001001_06101	F200W	CLEAR	FULL	1	5	1	64.421
jw01089001001_14101	F140M	CLEAR	FULL	1	5	1	64.421
jw01089001001_15101	F140M	GR150R	FULL	4	20	1	225.473
jw01089001001_16101	F140M	CLEAR	FULL	2	5	1	128.842
jw01089001001_17101	F140M	GR150C	FULL	4	20	1	225.473
jw01089001001_18101	F140M	CLEAR	FULL	1	5	1	64.421
jw01089001001_20101	F158M	CLEAR	FULL	1	5	1	64.421
jw01089001001_21101	F158M	GR150R	FULL	4	20	1	225.473
jw01089001001_22101	F158M	CLEAR	FULL	2	5	1	128.842
jw01089001001_23101	F158M	GR150C	FULL	4	20	1	225.473
jw01089001001_24101	F158M	CLEAR	FULL	1	5	1	64.421
Target: P330E, Observation / Visit 2							
jw01089002001_03102	F090W	GR150R	WFSS64R	2	10	5	37.672
jw01089002001_03104	F115W	GR150R	WFSS64R	2	10	5	37.672
jw01089002001_03106	F150W	GR150R	WFSS64R	2	10	5	37.672
jw01096002002_03108	F200W	GR150R	WFSS64R	2	10	5	37.672
Target: P330E, Observation / Visit 3							
jw01089003001_02107	F090W	GR150C	WFSS64C	2	5	2	37.474
jw01089003001_02105	F115W	GR150C	WFSS64C	2	5	2	37.474
jw01089003001_02103	F150W	GR150C	WFSS64C	2	5	2	37.474
Jw01089003001_02101	F200W	GR150C	WFSS64C	2	5	2	37.474

Since the star is too bright to be observed in the full array, the observations with P330E were done using the subarrays to avoid saturation (Figure 3). For the observations in the subarrays, target acquisition was done using the SOSSFAINT mode and the F480M filter. The exposure times were specified using the number of groups and integrations for all the observations as calculated using the JWST ETC to get several thousand counts in the first order of the trace without saturating. The total time for executing the NIS-015 program was 8.0 hours.

3 Data Processing

The data processing was done using the JWST calibration pipeline version 1.5.1. The *_uncal.fits* files for both the direct and the dispersed grism images were converted to rate images using the *Detector1* step of the pipeline. The bad-pixel mask generated from the commissioning data was used to identify and flag the bad pixels in this step. The direct images were processed through the *Image2* pipeline steps to assign WCS and do flat-fielding using the distortion reference files and flat-field reference files from the commissioning programs. The *Image3* pipeline step was used to create the source catalogs. The GR150R and C dispersed images were processed through the first few steps in the *Spec2* pipeline to assign WCS, apply flat-field correction and subtract background.

4 Analysis

The analysis for flux calibration was done using the drizzled grism images that combine all the dithered exposures for each grism. The direct image (single dither) taken at the start of the grism exposure sequence was used for creating the source catalog. The analysis steps performed on each filter + grism combination are listed below:

1. The detector positions (X,Y) from the source catalogs were used to locate the trace positions for the standard star and create a bounding box that encloses the 1st order trace. Since the offsets and extent for the spectral traces were close to that observed during the CV3 ground tests, we used the same information to determine the bounding boxes. The size of the bounding box varies with the length of the trace for each filter along the dispersion direction, and the extent of the PSF in the cross-dispersion direction is defined using an isophote which is 3-sigma above the source detection threshold. In the case of P330E, there is no direct image available. The offsets between the direct image, zero order, and higher spectral orders are assumed to be the same as for WD1657+343. The bounding box was specified manually in this case to be large enough to enclose the individual spectral orders.
2. Any remaining bad pixels or contaminating spectral orders of nearby sources inside the extraction box were masked. The masked pixels were replaced by interpolation from the neighboring pixels. The +1 order of the flux standards were fairly isolated and there was no significant contamination over the small apertures used for photometry.
3. Aperture photometry was performed on the 2D-cutouts that contain the 1st order trace using *photutils.aperture_photometry*. A rectangular aperture which is 2-pixel wide and with a height of 7 pixels was stepped along the spectral trace to perform the aperture photometry along the full length of the +1 order trace.

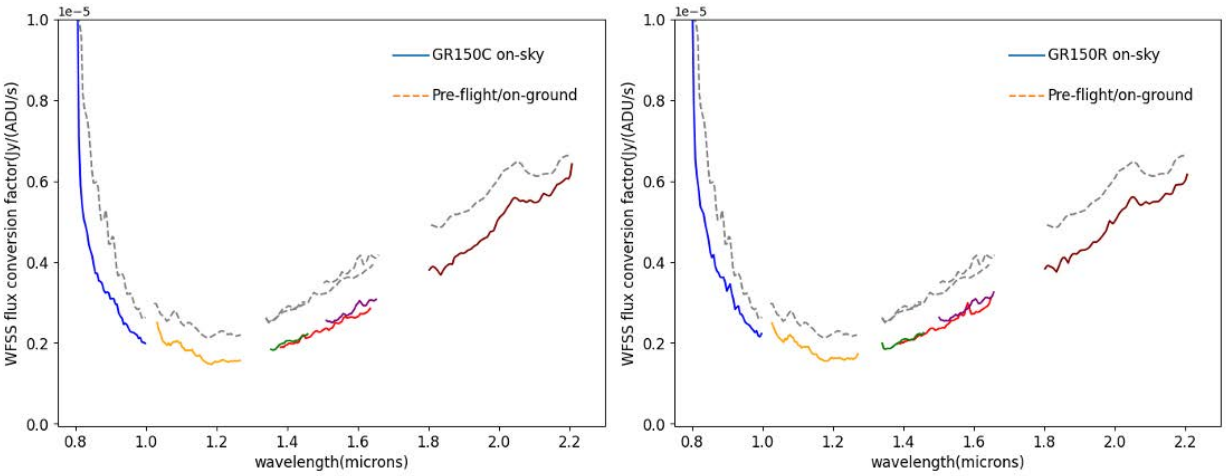

Figure 4: Plots showing the count rate (ADU/s) to flux (Jy) conversions over the range of NIRISS WFSS wavelengths for grisms GR150C (left) and GR150R (right) using WD1657+343 observations. The different segments show the different blocking filters. The counts to flux conversion factors from the pre-flight or on-ground measurements are also shown which are based on the assumed OTE transmission, grism+filter throughputs, and detector efficiencies.

4. The NIRISS WFSS dispersion solution from the wavelength calibration program NIS-016 (see Technical Report by Pacifici et al. 2022) was used to convert the results of photometry from counts/s as a function of position to counts/s as a function of wavelength.
5. The imaging programs from commissioning showed that the observed PSFs are almost identical to the model WebbPSFs (Perrin et al. 2014). So, the aperture corrections derived using the WebbPSF models were applied to convert the counts measured within a 7-pixel height rectangular aperture to the total counts for an infinite aperture.
6. The total counts were compared to the standard fluxes for the spectrophotometric calibration stars (CALSPEC, https://www.stsci.edu/hst/instrumentation/reference-data-for-calibration-and-tools/astronomical-catalogs/calspec). Specifically, for WD1657+343 we used the file *wd1657_343_stiswfcnic_004.fits*', and for P330E we used the file `*p330e_stiswfcnic_003.fits*'. The ratio of the fluxes (Jy) and counts/s give the conversion required to obtain the sensitivity.

The analysis steps listed above were repeated for all combinations of filters and GR150C and GR150R. The analysis was done for the FULL array using the star WD1657+343 and for the WFSS64R and WFSS64C subarrays using the star P330E. We found that the conversion factors determined using the two stars are consistent.

5 Results

5.1 Count rates to Flux Conversion Factor

In order to derive the WFSS sensitivity, we first derived the pixel counts (ADU/s) to flux (Jy) conversion factors as a function of wavelength for both the grisms. In Figure 4, the measured conversion factors derived using the standard star WD1657+343 are shown along with a comparison of the values used in the pre-flight photom reference files. The reference files for the

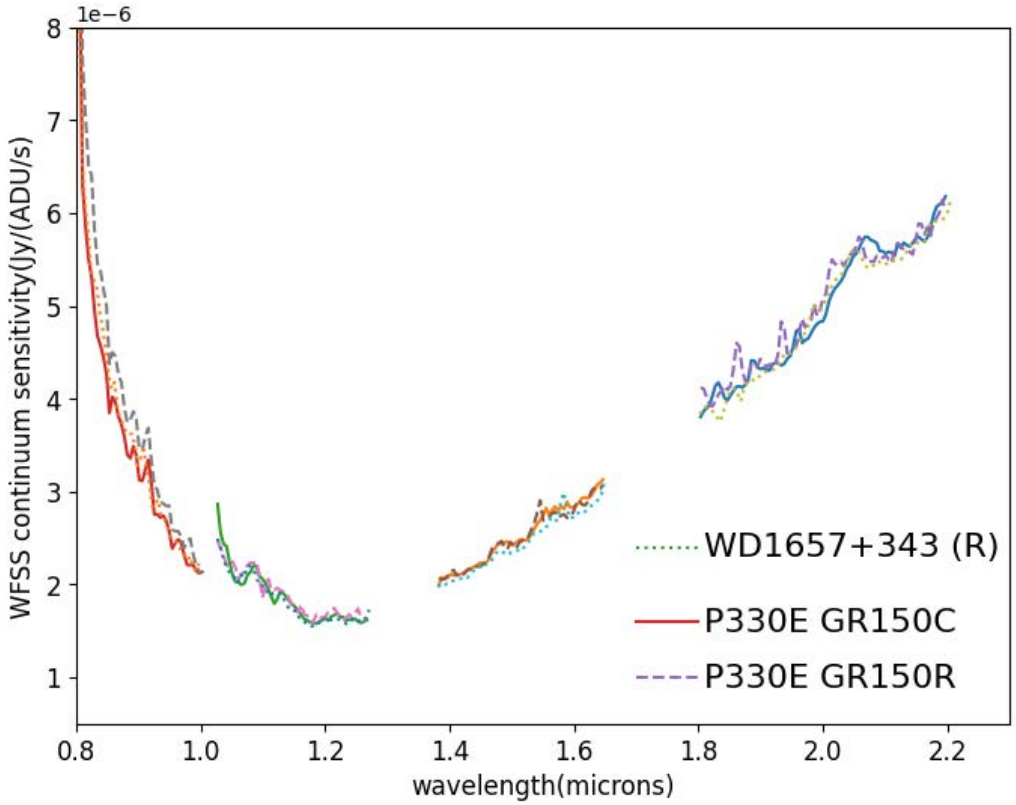

Figure 5: Plots showing the count rate (ADU/s) to flux (Jy) conversions over the range of NIRISS WFSS wavelengths for grisms GR150C and GR150R using P330E. Also shown for comparison are the results from the standard star WDS1657+343.

GR150R/C grisms that were delivered before the JWST launch were created using the trace measurements and wavelength calibrations (Ravindranath et al. 2014b,c) from the Cryo-Vac tests performed at the NASA GSFC. These tests were performed using a tungsten lamp as continuum source for the spectral trace and three monochromatic sources at specific wavelengths for wavelength calibration. However, no flux calibrations could be performed due to the lack of flux-

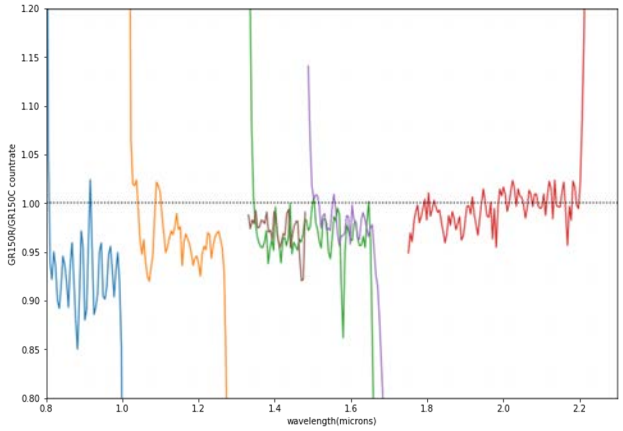

Figure 6: The ratio of the count-rates between the two grisms across the full wavelength range of NIRISS WFSS. The ratio of the countrates for the standard star WD1657+343 is shown here, and was also verified using the standard star P330E. The GR150C has ~ 5% higher throughput in the F090W filter compared to the GR150R grism.

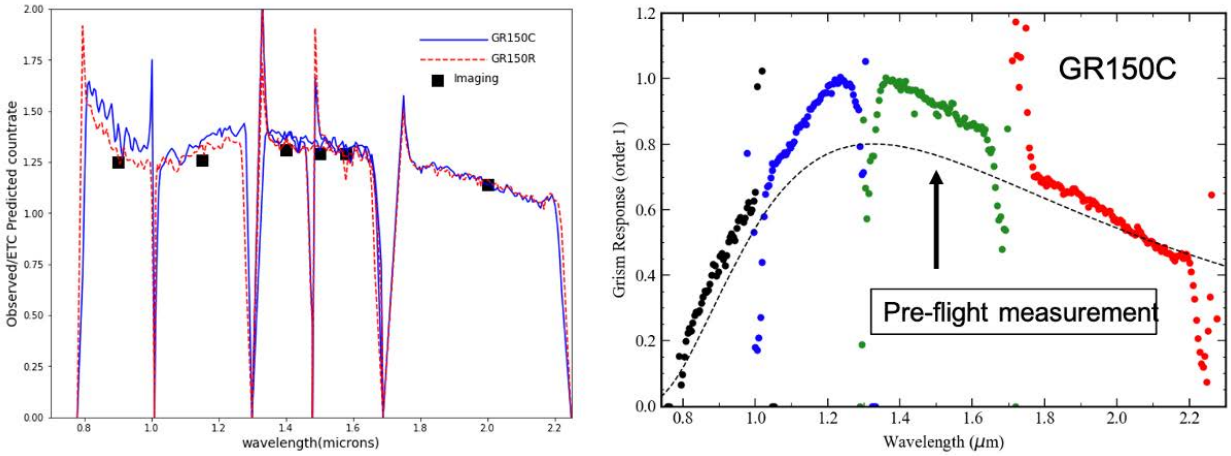

Figure 7: The ratio of observed count-rates to pre-flight ETC predictions are shown for the imaging filters and also crossed with GR150C/R grisms (left). The comparison of the GR150C grism throughput with the pre-flight measurements is also shown (right). The analysis of commissioning data clearly show that the actual observed throughput is 7- 20% of the pre-flight estimates over the wavelength range.

calibrated source that could be used for the ground tests. The pre-flight count rates were estimated based on estimates of the OTE throughput, filter+grism throughput, and detector response. The commissioning results show that the grisms have more efficiency than the pre-flight predictions in the sense that a lower flux can provide a count-rate of 1 ADU/s. This is true over the entire range of the WFSS wavelengths (0.8 – 2.2 microns). The count-rate to flux conversion was also checked using the standard star P330E using the grism exposures in WFSS64R subarray for the GR150R grism and the WFSS64C subarray for the GR150C grism. The results for P330E were found to be consistent with that obtained using WD1657+343 and a comparison is shown in Figure 5. The pre-flight WFSS reference files used in the JWST ETC and JWST pipeline assumed that the throughputs and efficiencies for the two grisms were the same. The performance observed during commissioning showed that the GR150C grism has better throughput in the blue than the GR150R grism. This is clearly visible in Figure 6 where we show the ratio of the count-rates for the same standard star (WD1657+343) observed in the two grisms. The ratio increases monotonically with wavelength showing the GR150C grism has higher throughput across the WFSS wavelength range. The GR150C grism offers about 2-5% better throughput at $\lambda > 1.0$ microns, and is ~5% better than GR150R grism at the short wavelengths $\lambda < 1.0$ microns.

The count rates from commissioning were also compared to the predictions from the ETC which are based on the pre-flight instrument performance based on throughputs for the components along the optical path and the detector efficiency, and found to be higher across the WFSS wavelength range. In Figure 7 we compare the observed count rate against the predicted count rates from the pre-flight ETC. The count rates for both imaging and WFSS modes are consistently > 7-20% of the pre-flight ETC predictions across the 0.8 – 2.2 microns wavelength range. The measured count rates also show good agreement between the imaging and WFSS commissioning observations, and the excess seen at < 1.0 micron for GR150C is due to the higher throughput (see Figure 6; Volk et al. 2022). The sensitivities from commissioning were compared to the pre-flight predictions from the ETC and are shown in Figure 8. The higher count rate in the WFSS mode as compared to the

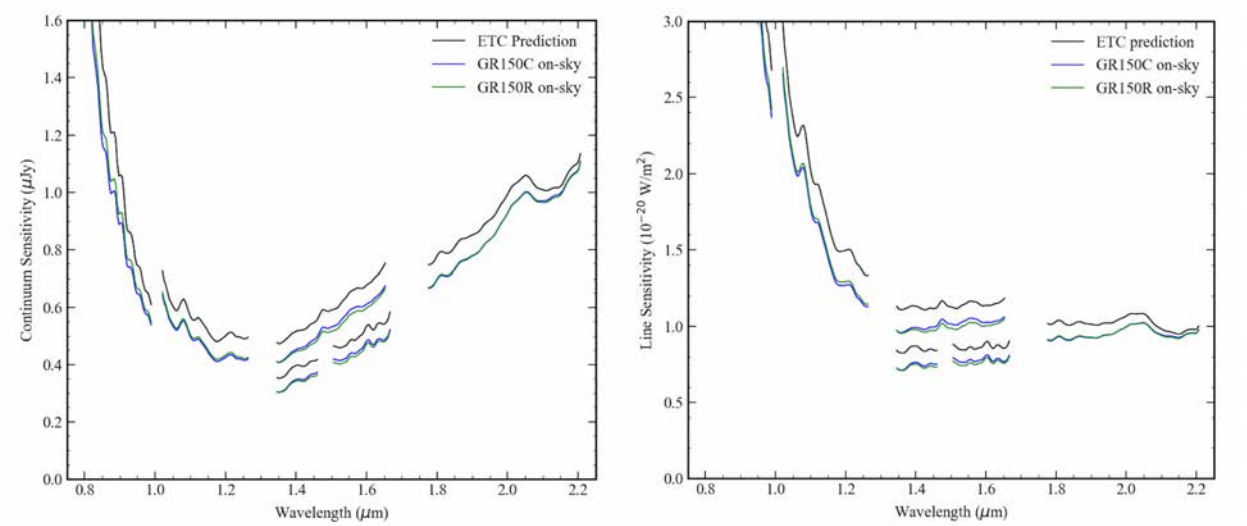

Figure 8: Plots showing the S/N = 10 continuum (left) and line flux sensitivity (right) for a 10ks observation using the GR150C/R grisms. Each segment corresponds to the blocking filters used in the WFSS mode. The predictions from ETC using pre-flight reference files is also shown.

pre-launch expectations means that the sensitivity of the WFSS mode, which is expressed as the flux density value required to produce S/N = 10 in a spectrum with 10,000s integration time, is better (lower value) than was predicted pre-launch. The NIRISS WFSS continuum sensitivity values were estimated using a theoretical S/N equation from Reike (2005), which allows for the estimated noise from the Poisson uncertainties of the source signal plus the per pixel combined noise with contributions from the sky background, from the dark current, and from the read-noise or other detector noise sources. Once the noise sources are specified the signal rate required to achieve the target S/N in a given time can be calculated. The calculation also makes a correction for the cosmic ray losses in the observations. The signal rate within the aperture of interest is then converted back to the total signal rate in an infinite aperture by applying appropriate aperture corrections. From the required signal rate, the WFSS pixel wavelength dispersion, the OTE mirror area, and the NIRISS photon conversion efficiency at a given wavelength the corresponding object brightness in Jansky can then be calculated to give the continuum sensitivity value as a function of wavelength.

The line sensitivity is calculated from the continuum sensitivity. It is assumed that the line emission is unresolved at the WFSS wavelength resolution and that it can be approximated as a 2-pixel box-car function. The line sensitivity is assumed to be the line flux value such that the line flux divided by the frequency interval of 2 pixels equals the continuum sensitivity in Jansky at each wavelength, or in other words the total flux from 2 pixels in the continuum sensitivity case equals the line flux from the same 2 pixels to get the same output S/N value. This calculation assumes that the spectral line has negligible underlying continuum contributing to the signal. The continuum and line flux that will give a signal-to-noise (S/N) = 10 in 10 kilo-seconds is shown in Figure 8. The on-sky sensitivities are better than the pre-flight ETC by 7 – 20% assuming a nominal 1.2 min Zodi background.

6 Reference File Creation

The results of the analysis from the commissioning program NIS-015 were used to create the *Photom* pipeline reference file for WFSS. The information for flux calibration for two grisms crossed with all the 6 blocking filters are provided in a single fits file (eg; *jwst_niriss_photom_0041.fits*). This reference file is used by the JWST calibration pipeline to apply the flux calibration in the photom step of the Calwebb_spec2 processing stage. For each filter and grism combination the photom file contains the scalar flux conversion constant *photmjsr* that converts the pixel counts to MegaJy/Steradian and its uncertainty, followed by arrays of wavelength and relative response (and the uncertainty) as a function of wavelength. The reference files were delivered to the JWST Calibration Reference Data System (CRDS) from where it is accessed by the JWST calibration pipeline.

7 References

Pacifici, C., et al., 2022, "NIRISS Commissioning Results: NIS-016 GR150C and GR150R Grism Wavelength Calibration", JWST Technical Report JWST-STScI-008296

Perrin, M. et al., 2014, ``Updated Point Spread Function simulations for JWST with WebbPSF'', Proc. SPIE, Vol. 9143, article id. 91433X

Ravindranath, S., 2014a, "NIRISS GR150R and GR150C Grism Calibration – Geometry of orders and Image Quality with Wavelength", JWST Technical Report JWST-STScI-003779

Ravindranath, S., 2014b, "NIRISS GR150R and GR150C Grism Calibration – Trace and Orientation", JWST Technical Report JWST-STScI-003780

Ravindranath, S., 2014c, "NIRISS GR150R and GR150C Grism Calibration – Wavelength Calibrations'', JWST Technical Report JWST-STScI-003781

Rieke, M., 2005, ``FGS/TFI Sensitivities'', JWST Technical Report JWST-CAL-003897

Volk, K., et al., 2022, "NIRISS On-Orbit Throughput Calibration", JWST Technical Report JWST-STScI-008268